



This is the accepted manuscript made available via CHORUS, the article has been published as:

## Effects of 3d and 4d transition metal substitutional impurities on the electronic properties of $\text{CrO}_2$

M. E. Williams, H. Sims, D. Mazumdar, and W. H. Butler

Phys. Rev. B **86**, 235124 — Published 17 December 2012

DOI: [10.1103/PhysRevB.86.235124](https://doi.org/10.1103/PhysRevB.86.235124)

# Effects of 3-d and 4-d-transition metal substitutional impurities on the electronic properties of CrO<sub>2</sub>

M. E. Williams,<sup>1</sup> H. Sims,<sup>2,3</sup> D. Mazumdar,<sup>2,3</sup> W.H.Butler<sup>2,3</sup>

*1. Department of Mathematics & Computer Science, University of Maryland Eastern Shore, Princess Anne, MD 21853*

*2. Center for Materials for Information Technology, University of Alabama, Tuscaloosa, AL 35401*

*3. Department of Physics, University of Alabama, University of Alabama, Tuscaloosa, AL 35401*

## **Abstract**

We present first-principles based density functional theory calculations of the electronic and magnetic structure of CrO<sub>2</sub> with 3d and 4d substitutional impurities. We find that the half-metallicity of CrO<sub>2</sub> remains intact for the ground state of all of the calculated substitutions. We also observe two periodic trends as a function of the number of valence electrons: if the substituted atom has six or fewer valence electrons, the number of down spin electrons associated with the impurity ion is zero, resulting in ferromagnetic alignment of the impurity magnetic moment with the magnetization of the CrO<sub>2</sub> host. For substituent atoms with eight to ten valence electrons (with the exception of Ni), the number of down spin electrons contributed by the impurity ion remains fixed at three as the number contributed to the majority increases from one to three resulting in antiferromagnetic alignment between impurity moment and host magnetization. In impurities with 7 valence electrons, the zero down spin and 3 down spin configurations are very close in energy. At 11 valence electrons, the energy is minimized when the substituent ion contributes 5 down-spin electrons. The moments on the 4d impurities, particularly Nb and Mo, tend to be delocalized compared those of the 3ds.

## **Introduction**

Rutile structure binary transition metal oxides (general formula  $XO_2$ ) comprise a very large family that covers much of the periodic table. Known stoichiometric rutile (or distorted rutile)  $XO_2$  compounds span the range from ions with nominal  $d^0$  configuration (X=Ti) to  $d^1$  (X=V, Nb, Ta) to  $d^2$  (X=Cr, Mo, W) to  $d^3$  (X=Mn, Tc, Re)  $d^4$  (X=Ru, Os), to  $d^5$  (X=Rh, Ir) to  $d^6$  (X=Pt) to  $d^{10}$  (X=Ge, Sn, Pb) [1]. The rutile-structure oxides show extremely diverse electronic properties. In the  $3d$  series,  $d^0$   $TiO_2$  is a non-magnetic insulator, whereas  $d^1$  vanadium oxide ( $VO_2$ ) is a strongly correlated oxide showing a metal-semiconductor transition concurrent with a rutile-monoclinic structural transition at  $\sim 340K$  [2]. Adding a single electron to  $VO_2$  (*i.e.*  $d^2$   $CrO_2$ ) reduces correlation effects and makes  $CrO_2$  a ferromagnetic (FM) half-metal with a gap in the minority spin channel [3]. As we progress to  $d^3$   $MnO_2$ , the system stabilizes in an antiferromagnetic (AFM) insulating state. However, in the  $4d$  (Mo, Tc, Ru, and Rh) and  $5d$  (Ta, W, Re, Os, Ir, Pt)  $XO_2$  oxides the correlated/semi-correlated behavior is almost lost and these oxides tend to be non-magnetic metals with a distorted structure [4]. The only exception to this trend is  $d^1$   $NbO_2$ , which is isoelectronic to  $VO_2$ , and exhibits a metal-insulator transition, again like  $VO_2$ .

Insight into the electronic properties can also be obtained through doping studies. In a previous work we investigated the case of Ru doping into half-metallic  $CrO_2$  [5]. We found that Ru formed localized states in the minority channel gap, but left the half-metallic feature of the electronic structure intact for low concentrations. In another study, we investigated the electronic and magnetic properties of Cr doped Vanadium oxide  $V_{1-x}Cr_xO_2$  [6], and found that the doped rutile-phase material remained ferromagnetic and half-metallic even for high concentrations. These intriguing results suggest the need for a systematic study of the doping

behavior of CrO<sub>2</sub>. The present work provides a first step in this direction which we hope will establish a basis for future experiments and theoretical insights.

We seek to answer the question of what happens when other *d* atoms are substituted into the half-metal CrO<sub>2</sub>. We speculate that almost all transition metal ions will substitute for Cr at least to some extent. Here we investigate systematically the effect of adding impurities in CrO<sub>2</sub> by substituting transition metal atoms from the *3d* and *4d* series for a Cr atom. In doing so, we explore the behavior of the additional electrons (or holes) provided by these impurity ions. For completeness we have considered all elements in the series even though some of the rutile phases (e.g. of FeO<sub>2</sub>, CoO<sub>2</sub>, and NiO<sub>2</sub>) have not been reported, suggesting that *high* concentration rutile-structure alloys of these elements with CrO<sub>2</sub> might not be stable. Our study is, however, aimed at understanding these materials for *low* impurity concentrations and at elucidating trends and qualitative physics.

## **Methodology**

We conducted first-principles based density function theory (DFT) calculations within the generalized gradient approximation (GGA) [7,8] using the Vienna *ab-initio* Simulation package (VASP) [9] and PAW pseudopotentials by Kresse and Joubert[10]. We constructed periodic supercells containing 24 atoms, *i.e.* 4 tetragonal 6-atom rutile cells having metal ions at the corners and body center. The supercell had dimensions  $2a \times b \times 2c$  and allowed us to substitute 12.5% of the Cr ions with the chosen impurity ion. All of the 8 sites within this supercell are equivalent for adding a single impurity. To check whether the 24 atom supercell was large enough for our purposes, we also calculated the electronic and magnetic structures of Nb and Ru impurities with a 48 atom supercell. The DOS changed in expected ways with localized impurity

states becoming narrower for the 48 atom cell compared to the 24 atom cell. Since this effect only reinforces our primary conclusion that impurity states that form within the gap do not destroy the half-metallicity, we tentatively conclude that larger cells do not add sufficient additional information to justify their use in this survey.

In all calculations, we used a 5 x 9 x 7 Monkhorst-Pack [11] k-point grid and a plane wave cutoff of 400 eV. We allowed structural relaxation of the supercell but did not allow for the possibility of complicated extended defects in the rutile structure which might include deviations from oxygen stoichiometry. In all of our supercells, the number of O anions was twice the number of cations.

At the suggestion of reviewers, we considered the possibility that the substituted cation might prefer an “interstitial” site, i.e. some site other than the one vacated by the Cr ion that was removed from the cell. We concluded that this is unlikely based on the following considerations: Je and Sinnott investigated Frenkel and Schottky defects in  $\text{TiO}_2$  [12] and found that Schottky defects were unstable by energies ranging from 3.5 to 5.5 eV depending on the model while Frenkel defects were unstable by 2 to 4 eV. The lowest energy Frenkel defect consisted of a displacement of one of the Ti ions to a position at the center of an a-c face of the standard tetragonal rutile cell.

We investigated a Ru ion as a Frenkel defect in a 48 atom  $\text{CrO}_2$  supercell, displacing the Ru ion to the center of an a-c face of the standard tetragonal cell corresponding to the lowest energy defect found in ref. [12]. After structural relaxation, which left the basic structure of the cell intact with a vacancy at the position from which the Cr ion was removed, the energy was

compared to the energy of the relaxed structure with the Ru ion at the position originally occupied by the Cr ion. The Frenkel defect configuration was 4.4eV higher in energy.

The initial parameters of the cells used for the substitutional impurity studies were based on the known bulk CrO<sub>2</sub> values ( $a=b=0.4593\text{nm}$ ,  $c=0.2959\text{nm}$ ). Each system was relaxed so that the interatomic forces were less than 0.1 eV/Å, before the electronic structure and magnetic moments were calculated.

Plane wave based DFT codes generate charge and magnetization densities that extend throughout the computational cell. Any method of assigning a charge or magnetic moment to a particular ion is, to some extent, arbitrary. The total change in the spin-magnetic moment on substituting an impurity atom for a Cr atom is, however, well and unambiguously defined. In these particular systems, moreover, we find that the minority Fermi energy continues to lie in a gap in the density of states even after the substitution. This implies that the number of minority electrons in the cell is an integer. Since the total number of electrons in the cell is also an integer, it follows that the number of majority electrons is an integer and finally that the total spin moment of the cell after the substitution is an integer. Thus, if we assign a moment of  $2\mu_B$  to each of the Cr ions, we can associate the difference between the total cell moment after substitution and  $2n\mu_B$  with the impurity moment. Here  $n$  is the number of Cr ions in the cell after the substitution ( $n=7$  for the calculations based on the 24 atom cell reported here). When we report magnetic moments for individual ions, they are calculated within a sphere of radius 0.9 Å for the 3d ions and 1.0 Å for the 4d ions. We find that the orbital moment is less than  $0.05\mu_B$  for both the Cr and impurity ions, and we neglect its contribution in the following.

## **Results**

## Electronic Structure of CrO<sub>2</sub>

It is helpful to briefly review the DFT-GGA electronic structure of CrO<sub>2</sub> which we used as a starting point for understanding the effect of placing impurities into this host. The density of states (DOS) is shown in Figure 1 where the O-*p* states and Cr-*d* states are labeled. The assignment of states to Oxygen or Cr ions is, of course, approximate since all of the states are hybridized and the charge and magnetization densities from a DFT calculation cannot be assigned unambiguously to a particular ion. The number of states per atom or a given orbital type, however, is largely conserved by the hybridization so that it is possible to describe the electronic structure in a manner that is consistent with a chemical picture.

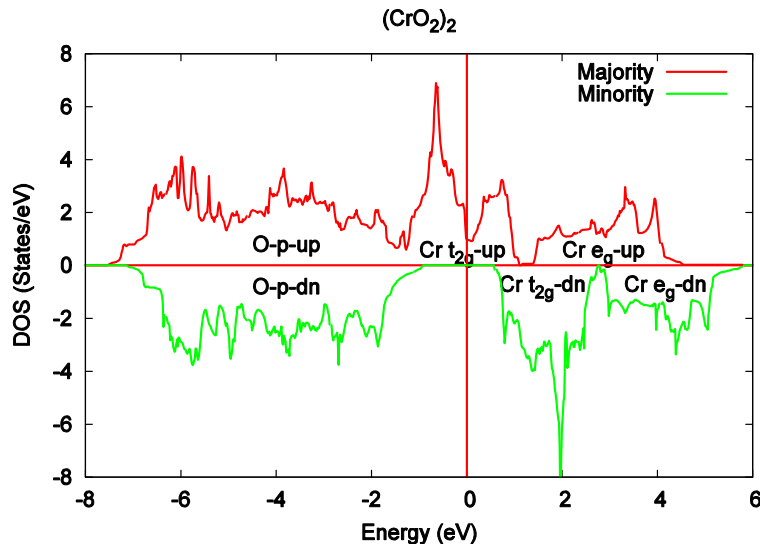


**Figure 1. Electronic Density of States of CrO<sub>2</sub>.**

In this picture, the oxygen *p*-states are filled by each oxygen ion acquiring 2 additional electrons from the Cr ions. Since there are twice as many O ions as Cr ions, the O ions will be in the (nominal) -2 valence state and the Cr ions will be in the (nominal) +4 valence state. Each Cr ion is surrounded by 6 O ions which form a distorted octahedron. The approximate cubic crystal symmetry of the distorted octahedron breaks up the 5 Cr *d*-states per spin into a lower energy

group of 3 per Cr ion that would be labeled “ $t_{2g}$ ” if the symmetry were exactly cubic and a corresponding higher energy group of 2 “ $e_g$ ” states per Cr ion. This is most easily seen for the minority Cr-d DOS where the DOS vanishes at an energy that separates a “lump” of DOS that contains 3 electrons from one that contains 2 electrons. For the majority channel, the strong exchange interactions push the majority “ $t_{2g}$ ” states down in energy so that they overlap slightly with the majority O-p states. In a tight-binding model, this overlap between the O-p and Cr-d majority states requires some degree of direct Cr-d to Cr-d interaction. This is possible in the rutile structure because of the relatively small Cr-Cr distance along the c-axis (equal to the c-axis lattice parameter).

The DFT-GGA DOS for non-magnetic  $\text{CrO}_2$  is very similar to the magnetic version with the exception that the majority  $d$ -states are higher (identical to the minority) and well separated from the O- $p$  states. The Fermi energy falls such that 1 majority and 1 minority Cr- $d$  state are occupied. Thus in DFT, the system reduces its energy by generating spin-polarization that allows it to push 2 occupied Cr-d states down in energy and simultaneously push the unoccupied  $d$ -states up. The spin-polarized system gains an additional reduction in energy because the majority Fermi energy falls in a pseudo-gap that forms within the “ $t_{2g}$ ” complex.

### **$d^0$ Cr(Ti)O<sub>2</sub> and Cr(Zr)O<sub>2</sub>**

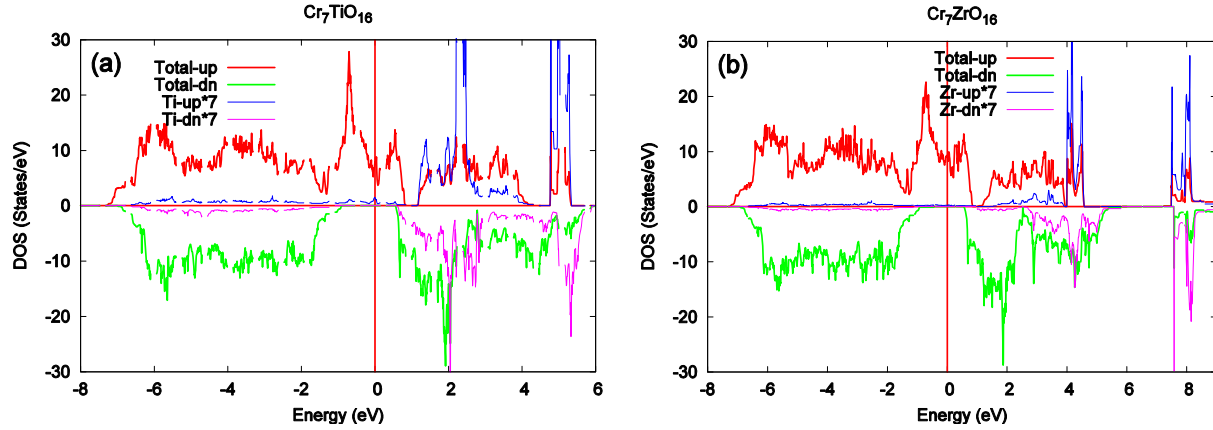
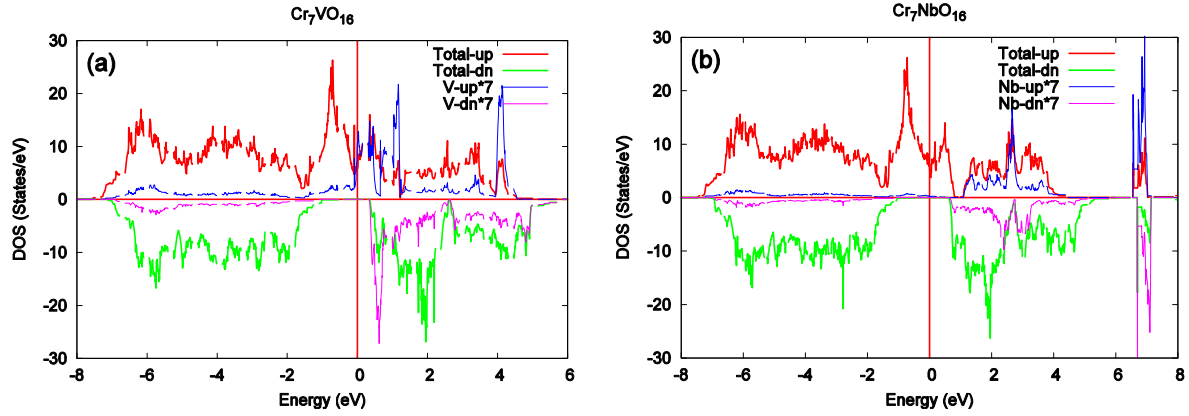


Figure 2. (color online) Calculated DOS for (a) Ti and (b) Zr impurities in  $\text{CrO}_2$ . The total DOS in the 24 atom supercell is indicated by thick lines. The DOS for the Ti and Zr impurities is indicated by thinner lines. The impurity DOS has been multiplied by 7 to enhance visibility. The impurity DOS is calculated within a sphere of radius 0.9 Å.

Figure 2 shows the calculated DOS for Ti and Zr impurities in  $\text{CrO}_2$ . Since both impurity ions are surrounded by 6 oxygen ions, they are in a +4 valence state ( $d^0$  configuration), the net moment on the Ti or Zr site is expected to be 0 so that each substituted Ti or Zr reduces the magnetic moment by  $2\mu_B$ . This is in qualitative agreement with our calculations. The net decrease in spin-moment associated with either substitution is exactly  $2\mu_B$ . This is clear from the DOS curves. Because the minority band gap is still present and the Fermi energy falls in it, the spin-moment is an integer and, because the number of occupied minority states does not change on substitution (the occupied minority states consist of the O  $3-p$  states), all of the change in the number of electrons (-2 per substitution) must be accommodated in the majority channel. The moment within 0.9Å radius spheres surrounding the Ti or Zr sites is not exactly zero, but 0.105 for Ti and 0.03 for Zr.

One major difference between Ti and Zr is in the unoccupied part of the DOS where it can be seen that the Zr impurity  $d$ -states lie much higher in energy than those of Ti and have a larger splitting between the “ $t_{2g}$ ” and “ $e_g$ ” states. Another difference is that there is stronger hybridization of the Ti- $d$  states with the Oxygen- $p$  states due to their closer proximity in energy.

## $d^1$ Cr(V)O<sub>2</sub> and Cr(Nb)O<sub>2</sub>



**Figure 3. (Color online)** Calculated DOS for (a) V and (b) Nb impurities in CrO<sub>2</sub>. The total DOS in the 24 atom supercell is indicated by thick lines. The DOS for the V and Nb impurities is indicated by thinner lines and has been multiplied by 7. The impurity DOS is evaluated within a sphere of radius 0.9Å centered on the impurity site.

Figure 3 shows the calculated DOS for V and Nb impurities in CrO<sub>2</sub>. Both of these impurity atoms have 5 valence electrons, one less than the Cr atom that they replace, so that when they are ionized by the quasi-octahedral oxygen environment, their configuration is expected to become  $d^1$ . We find that the total spin moment of the cell after the substitution is reduced from 16 to 15 indicating that the “V moment” and the “Nb moment” have aligned ferromagnetically with the magnetization of the host. The use of quotes in the preceding sentence is intended to indicate that the common notion of the spin moment “on” a transition metal ion may be an oversimplification, at least within this type of mean field calculation. For CrO<sub>2</sub>, the moment within a 0.9Å radius Cr sphere is 1.796 or 90% of the total moment per Cr ion (with nominal spin  $2\mu_B$ ). For the V impurity, the sphere moment is  $0.455 \mu_B$  or 45.5% of its nominal spin and for Nb it is only  $0.069 \mu_B$  or less than 7%.

We can obtain a qualitative understanding of the apparent missing magnetic moment from the information listed in Tables I and II. For the cell with the Nb substitution, the average spin

moment within the 6 O ion spheres (radius 1.45Å) increases from 0.0105 $\mu_B$  to 0.0465  $\mu_B$ . This would account for 0.22  $\mu_B$ . The average moment within the 7 Cr spheres increases from 1.796  $\mu_B$  to 1.883  $\mu_B$ . This is sufficient to account for 0.61  $\mu_B$ . It should be noted that the sum of the sphere moments will not in general equal the total cell moment, but it is clear that the magnetization associated with the Nb substitution is quite diffuse.

The situation is similar for the V impurity, if less dramatic. In addition to the 0.455  $\mu_B$  within the V sphere, the average moment of the 6 neighboring O ions increases from 0.0105 to 0.0127 accounting for 0.013  $\mu_B$ . The moment within the 7 Cr spheres increases from 1.796  $\mu_B$  to 1.851  $\mu_B$  accounting for 0.385  $\mu_B$ .

### $d^2$ Cr(Mo)O<sub>2</sub>

Figure 4 shows the calculated DOS for a Mo impurity in CrO<sub>2</sub>. Mo is iso-electronic with Cr. Both atoms have 6 valence electrons. Their ions in the octahedral O environment are expected to be in the  $d^2$  state. The calculated magnetic moment of 16 $\mu_B$  for the Cr<sub>7</sub>MoO<sub>16</sub> supercell is consistent with this state picture. However, from Figure 4 it appears that Mo is in something

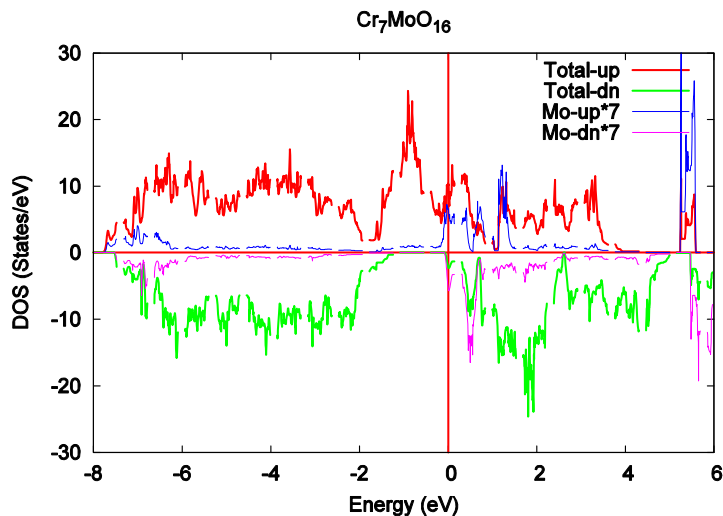


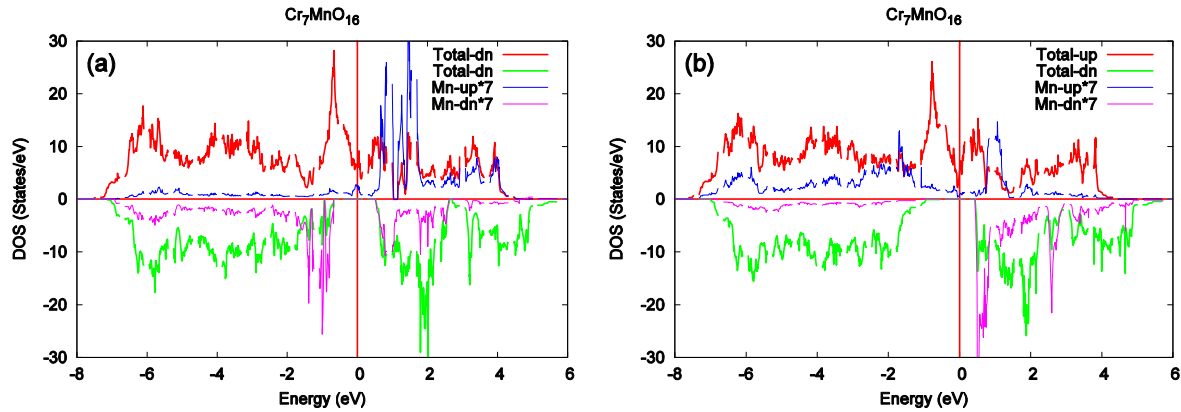
**Figure 4. (Color online) Calculated DOS for Mo impurity in CrO<sub>2</sub>. The total DOS in the 24 atom supercell is indicated by thick lines. The DOS for the Mo impurity site is indicated by thinner lines and has been multiplied by 7. The impurity DOS is evaluated within a sphere of radius 0.9Å centered on the impurity site.**

closer to a  $d^0$  state since less than 12.5% of the expected  $2\mu_B$  is within the 0.9Å radius sphere.

This picture is also supported by the increased moment on the O ions surrounding the Mo impurity and by the enhancement of the moments within the Cr ion spheres as shown in Tables I and II.

From Figure 4, it is also clear that the shift of the impurity 4d-states to higher energy compared to 3d is reduced in Mo compared to Nb. The Mo minority impurity “ $t_{2g}$ ” states lie just above the Fermi energy so that the system is only barely a half-metal. There is a large splitting between the “ $t_{2g}$ ” and “ $e_g$ ” impurity states.

### $d^3$ Cr(Mn)O<sub>2</sub> and Cr(Tc)O<sub>2</sub>



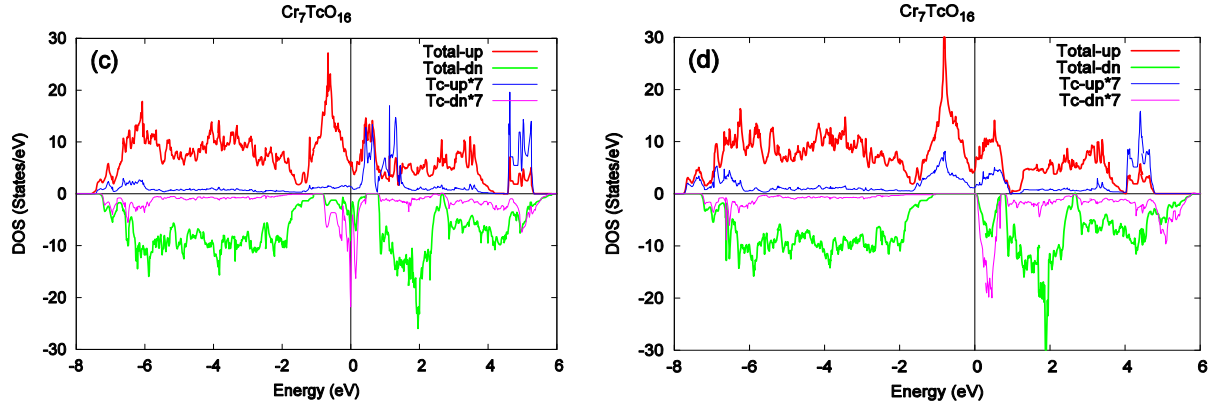


**Figure 5. (Color online)** Calculated DOS for Mn and Tc impurities in  $\text{CrO}_2$ . (a) Solution to DFT-GGA equations for Mn impurity with total moment per cell of  $11\mu_B$  and (b)  $17\mu_B$ . (c) Solution to DFT-GGA equations for Tc impurity with total moment per cell of (c)  $13.5\mu_B$  and (d)  $17\mu_B$ . The total DOS in the 24 atom supercell is indicated by thick lines. The DOS for the Mn impurity site is indicated by thinner lines and has been multiplied by 7. The impurity DOS is evaluated within a sphere of radius  $0.9\text{\AA}$  centered on the impurity site.

Figure 5 shows the calculated DOS for a Mn impurity ((a) and (b)) and for a Tc impurity ((c) and (d)) in our 24 atom supercell. For all substitutions, we searched for both ferromagnetic (impurity moment aligned with host moments) and antiferromagnetic (impurity moment anti-aligned with host moments) solutions to the DFT-GGA equations. For the impurities presented in Figures 1-4, we were only able to obtain one solution for each impurity. For Mn and Tc impurities, however, we were able to obtain multiple solutions. For Mn, the two quite different solutions appear to be nearly degenerate in energy. One solution (panel a) generates a low moment. For this case we find a total cell moment of  $11\mu_B$ , i.e. a net decrease of  $5\mu_B$  on substitution of a Cr atom by a Mn atom. Since a  $\text{Mn}^{4+}$  ion is expected to be in the  $d^3$  state, we would naturally associate the decrease of  $5\mu_B$  with a Mn ion having a moment of  $3\mu_B$  aligned antiferromagnetically. This is qualitatively what our calculation describes. The moment within the  $0.9\text{\AA}$  radius sphere is  $-2.17\mu_B$  rather than  $-3$ , but as we have emphasized the sphere radius is somewhat arbitrary. Part of the difference, is no doubt related to the strong hybridization of the

minority Mn-d states with the O-p states that can be seen in Figure 5a. This picture is supported by the calculated moments within the O-ion spheres (radius=1.45Å) which average  $-0.026 \mu_B$  on the 6 O-ions surrounding the Mn ion compared to  $+0.0105 \mu_B$  for the O spheres in CrO<sub>2</sub>. It is remarkable that if the two Mn impurity solutions are indeed within 3meV in energy with the antiferromagnetic phase lower in energy as we have calculated, it should be (barely) possible to effect a transition with a 9T laboratory magnet.

The other solution that we found (Figure 5b) gave a total cell moment of  $17\mu_B$  and was calculated to be approximately 3meV higher in energy than the  $11 \mu_B$  solution. The natural interpretation would be that in this case, the Mn d<sup>3</sup> ion with a spin moment of  $3\mu_B$  is aligned ferromagnetically with the host spin moments. This picture is consistent with the calculated moment within the (0.9Å radius) sphere of  $2.52 \mu_B$ . Experimental observation of a marked decrease in magnetization with Mn substitution [13] supports our picture of a large negative moment on the Mn ion.

We also found two solutions for the Tc impurity. When the DFT-GGA equations are solved using VASP and following normal procedures beginning with a local impurity moment that is either aligned or anti-aligned one obtains a solution with a moment of approximately  $13.5 \mu_B$ . For this solution (Figure 5c), the impurity “t<sub>2g</sub>” states sit astride the Fermi energy and are approximately half-filled. We searched for additional states with 11 or  $17 \mu_B$  per cell corresponding to anti-ferromagnetic or ferromagnetic alignment of the impurity moment using a feature of VASP that allows one to constrain the total cell moment. Solutions with  $11\mu_B$  were not stable when the constraint was removed, but solutions with  $17 \mu_B$  were stable (Fig. 5d) and were lower in energy than the  $13.5 \mu_B$  solution (Fig 5c) by 173meV.

## $d^4$ Cr(Fe)O<sub>2</sub> and Cr(Ru)O<sub>2</sub>

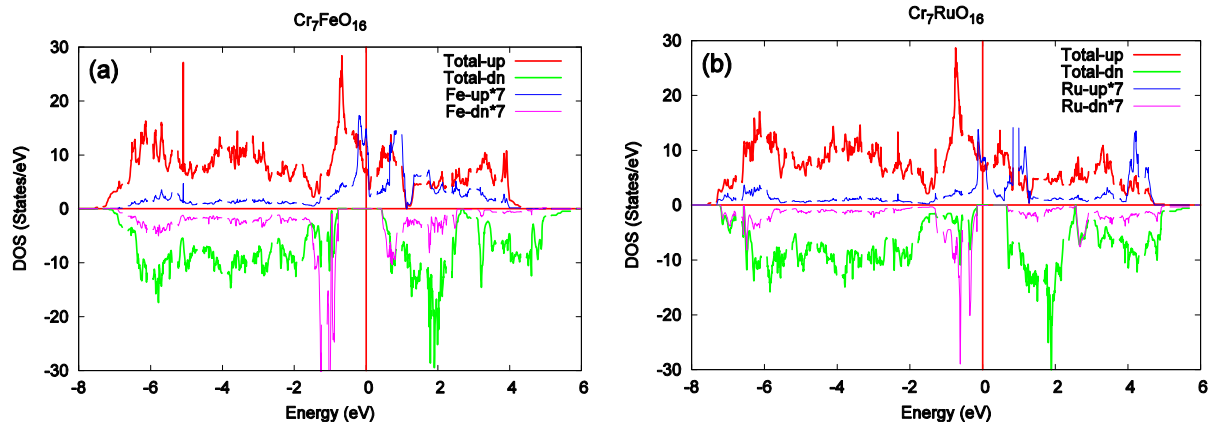
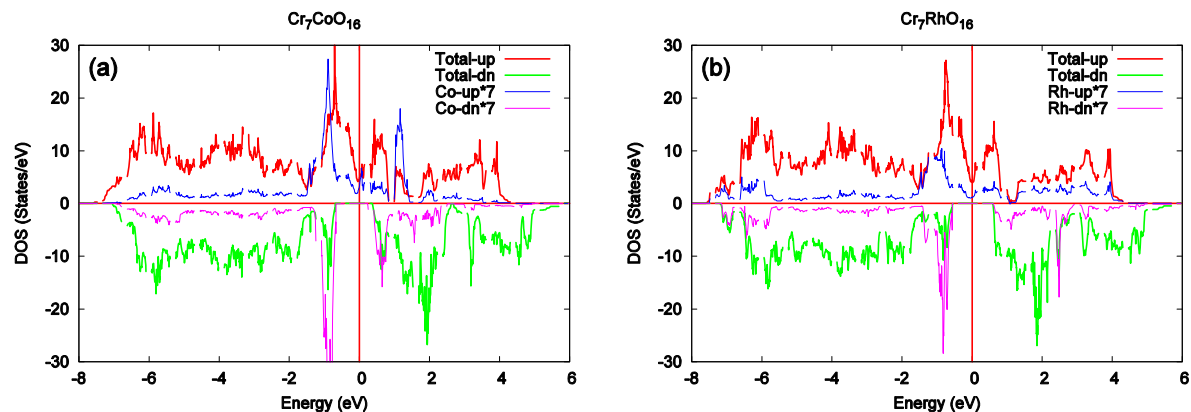


Figure 6. . (Color online) Calculated DOS for (a) Fe and (b) Ru impurities in CrO<sub>2</sub>. The total DOS in the 24 atom supercell is indicated by thick lines. The DOS for the Fe and Ru impurities is indicated by thinner lines and has been multiplied by 7. The impurity DOS is evaluated within a sphere of radius 0.9 Å centered on the impurity site.

Figure 6 shows the DOS for (a) an Fe impurity and (b) a Ru impurity in CrO<sub>2</sub>. Fe and Ru each have 8 valence electrons so their 4+ ions will have 4 electrons. The net change in moment due to the substitution is  $-4\mu_B$  in both cases. From the DOS it is clear that this is accomplished by the three minority  $t_{2g}$  states moving below the Fermi energy. For Fe, the impurity minority  $t_{2g}$  states are moved down to the top of the O-p states so that the band gap is not greatly reduced from that of CrO<sub>2</sub>. For Ru, on the other hand, the occupied minority  $t_{2g}$  states are in the gap and significantly reduce it.

## $d^5$ Cr(Co)O<sub>2</sub> and Cr(Rh)O<sub>2</sub>



**Figure 7. (Color online) Calculated DOS for (a) Co and (b) Rh impurities in  $\text{CrO}_2$ . The total DOS in the 24 atom supercell is indicated by thick lines. The DOS for the Co and Rh impurities is indicated by thinner lines and has been multiplied by 7. The impurity DOS is evaluated within a sphere of radius  $0.9\text{\AA}$  centered on the impurity site.**

Figure 7 shows the DOS for Co and Rh impurities in  $\text{CrO}_2$ . Co and Rh would have a  $d^5$  configuration as  $4+$  ions. Similarly to Fe and Ru, for Co and Rh, the minority “ $t_{2g}$ ” states are occupied. In both cases they are shifted down to the top of the minority O-p bands so that sizable minority band gaps survive the substitution.

### $d^6$ Cr(Ni)O<sub>2</sub> and Cr(Pd)O<sub>2</sub>

Figure 8 shows the calculated DOS for Ni and Pd impurities in  $\text{CrO}_2$ . Ni and Pd impurities are expected to be in the  $d^6$  configuration. If they follow the rule of filling the 3 minority “ $t_{2g}$ ” states, these ions would contribute no magnetization to the cell so that the total moment would decrease by  $2\mu_B$  per impurity. That is what happens for the Pd impurity. The three minority “ $t_{2g}$ ” states are filled and the two minority “ $e_g$ ” states are empty. The three minority states induced by the impurity must be compensated by the remaining three electrons contributed by the Pd ion so that the total moment induced by the impurity is simply  $-2\mu_B$ , i.e. the moment that would have been contributed by the replaced Cr ion. For Ni, the case is somewhat different. The “ $e_g$ ” levels

are split with one “ $e_g$ ” level being filled and the other empty. This leads to 4 minority electrons per impurity and 2 majority, so that the total moment induced by the impurity is  $-3\mu_B$ .

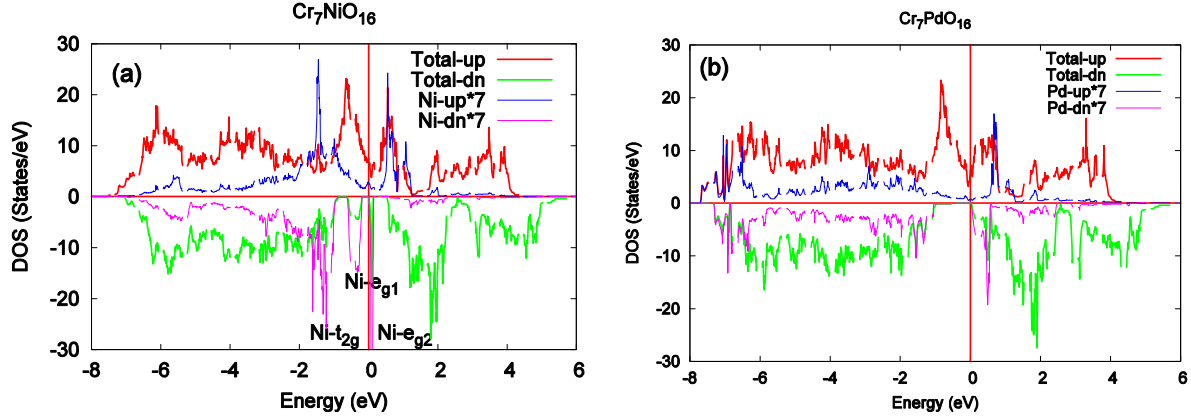


Figure 8. (Color online) Calculated DOS for (a) Ni and (b) Pd impurities in  $\text{CrO}_2$ . The total DOS in the 24 atom supercell is indicated by thick lines. The DOS for the Ni and Pd impurities is indicated by thinner lines and has been multiplied by 7. The impurity DOS is evaluated within a sphere of radius  $0.9\text{\AA}$  centered on the impurity site.

Consider adding an additional electron to the DOS of Figure 7. One way that it can be done is exemplified by Pd, which simply adds it to the majority, pulling the majority states down slightly relative to the minority to accommodate the additional electron. The system with a Ni impurity adds the electron in a different way by distorting the octahedron so that the cation to apical O distances are increased from  $1.91\text{\AA}$  to  $1.99\text{\AA}$ . This causes the two “ $e_g$ ” states to split. The system can then occupy the lower one and reduce its energy. This “strategy” works much better for Ni than for Pd because the Ni impurity “ $e_g$ ” states have moved into the gap which makes them very narrow. It can be shown that because they are in the gap, they would be delta-functions if there were only interactions between the Cr ions and their surrounding O ions. In fact, there is significant direct interaction between neighboring Cr ions in the direction of the c axis. One of the “ $e_g$ ” orbitals, however is oriented orthogonal to this direction so it is extremely

narrow. The splitting of the “ $e_g$ ” states in the  $\text{CrO}_2$  gap is an example of a Jahn-Teller distortion [14].

### $d^7$ $\text{Cr}(\text{Cu})\text{O}_2$ and $\text{Cr}(\text{Ag})\text{O}_2$

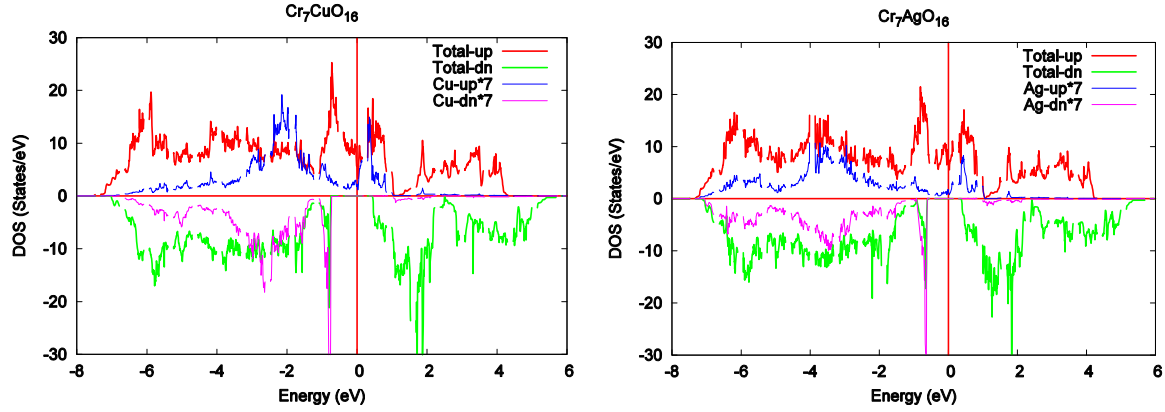


Figure 9. (Color online) Calculated DOS for (a)Cu and (b) Ag impurities in  $\text{CrO}_2$ . The total DOS in the 24 atom supercell is indicated by thick lines. The DOS for the Cu and Ag impurities is indicated by thinner lines and has been multiplied by 7. The impurity DOS is evaluated within a sphere of radius  $0.9\text{\AA}$  centered on the impurity site.

The DOS for Cu and Ag impurities in  $\text{CrO}_2$  is shown in Figure 9. Cu and Ag are expected to be in the  $d^7$  configuration as impurities in  $\text{CrO}_2$ . From Figure 9, it is clear that they prefer to have all of their minority d-states occupied. In both cases the minority impurity  $t_{2g}$  states hybridize strongly with the O-p states. The minority “ $e_g$ ” states remain in the gap and occupy a very narrow energy range. Since five of the seven electrons of the  $d^7$  ions go into the minority, the net change in magnetization induced by a Cu or Ag substitution is  $-5\mu_B$ , consisting of the loss of the two majority electrons “on” the Cr ion and the net three minority electrons “on” the Cu or Ag ions.

Table I: Summary of magnetic moment values for  $3d$  substitution of  $\text{CrO}_2$ . Up (down) implies ferromagnetic (anti-ferromagnetic) alignment with host Cr. The magnetic moment units are  $\mu_B$ .

| Element  | Ti             | V              | Cr             | Mn                              | Fe             | Co             | Ni             | Cu             |
|--|----------------|----------------|----------------|---------------------------------|----------------|----------------|----------------|----------------|
| Nominal spin configuration of impurity           | 0 up<br>0 down | 1 up<br>0 down | 2 up<br>0 down | 3 up / 0 dn<br>or<br>0 up/ 3 dn | 1 up<br>3 down | 2 up<br>3 down | 2 up<br>4 down | 2 up<br>5 down |
| Total cell moment ( $\mu_B$ )                    | 14             | 15             | 16             | 17 or 11                        | 12             | 13             | 12             | 11             |
| Impurity moment ( $\mu_B$ )                      | 0.10           | 0.46           | n/a            | 2.52 FM -<br>2.17 AF            | -1.27          | -0.17          | -0.52          | -0.60          |
| Average Cr moment ( $\mu_B$ )                    | 1.79           | 1.85           | 1.80           | 1.80 FM<br>1.76 AF              | 1.77           | 1.73           | 1.66           | 1.59           |
| Average O moment ( $\mu_B$ )                     | 0.00           | 0.00           | 0.01           | 0.02 FM<br>-0.01 AF             | -0.02          | -0.02          | -0.03          | -0.04          |
| Average moment of O nearest impurity ( $\mu_B$ ) | 0.02           | 0.02           | n/a            | 0.05 FM -<br>0.03 AF            | -0.04          | -0.04          | -0.05          | -0.09          |
| Distance to apical O ( $\text{\AA}$ )            | 1.97           | 1.93           | 1.91           | 1.90                            | 1.89           | 1.89           | 1.99           | 2.02           |
| Distance to planar O ( $\text{\AA}$ )            | 1.96           | 1.88           | 1.91           | 1.90                            | 1.88           | 1.90           | 1.89           | 2.01           |

Table II: Summary of magnetic moment values for 4d substitution of CrO<sub>2</sub>. Up (down) implies ferromagnetic (anti-ferromagnetic) alignment with host Cr. The magnetic moment units are  $\mu_B$ .

| <b>Element</b>   | <b>Zr</b>              | <b>Nb</b>              | <b>Mo</b>              | <b>Tc</b>              | <b>Ru</b>              | <b>Rh</b>              | <b>Pd</b>              | <b>Ag</b>              |
|--|------------------------|------------------------|------------------------|------------------------|------------------------|------------------------|------------------------|------------------------|
| <b>Nominal spin configuration of impurity</b>                    | <b>0 up<br/>0 down</b> | <b>1 up<br/>0 down</b> | <b>2 up<br/>0 down</b> | <b>3 up<br/>0 down</b> | <b>1 up<br/>3 down</b> | <b>2 up<br/>3 down</b> | <b>3 up<br/>3 down</b> | <b>2 up<br/>5 down</b> |
| <b>Total cell moment (<math>\mu_B</math>)</b>                    | <b>14</b>              | <b>15</b>              | <b>16</b>              | <b>17</b>              | <b>12</b>              | <b>13</b>              | <b>14</b>              | <b>11</b>              |
| <b>Impurity moment (<math>\mu_B</math>)</b>                      | <b>0.03</b>            | <b>0.07</b>            | <b>0.27</b>            | <b>1.08</b>            | <b>-0.93</b>           | <b>-0.21</b>           | <b>0.13</b>            | <b>-0.36</b>           |
| <b>Average Cr moment (<math>\mu_B</math>)</b>                    | <b>1.79</b>            | <b>1.88</b>            | <b>1.94</b>            | <b>1.90</b>            | <b>1.77</b>            | <b>1.75</b>            | <b>1.77</b>            | <b>1.56</b>            |
| <b>Average O moment (<math>\mu_B</math>)</b>                     | <b>-0.01</b>           | <b>0.02</b>            | <b>0.02</b>            | <b>0.02</b>            | <b>-0.04</b>           | <b>-0.03</b>           | <b>-0.00</b>           | <b>-0.05</b>           |
| <b>Average moment of O nearest impurity (<math>\mu_B</math>)</b> | <b>0.03</b>            | <b>0.05</b>            | <b>0.04</b>            | <b>0.08</b>            | <b>-0.07</b>           | <b>-0.04</b>           | <b>-0.02</b>           | <b>-0.09</b>           |
| <b>Distance to apical O (<math>\text{\AA}</math>)</b>            | <b>2.09</b>            | <b>2.01</b>            | <b>1.96</b>            | <b>1.95</b>            | <b>1.97</b>            | <b>1.98</b>            | <b>2.00</b>            | <b>2.15</b>            |
| <b>Distance to planar O (<math>\text{\AA}</math>)</b>            | <b>2.09</b>            | <b>1.9</b>             | <b>1.94</b>            | <b>1.96</b>            | <b>1.98</b>            | <b>2.00</b>            | <b>2.02</b>            | <b>2.16</b>            |

## Moment Rule

Within DFT-GGA, the following rule appears to govern the ground state magnetic moment for  $3d$  and  $4d$  transition metal impurities in  $\text{CrO}_2$ : The number of minority electrons added by the impurity increases from zero (Ti, Zr, V, Nb, Cr, Mo, Mn, Tc) to three (Mn, Fe, Ru, Co, Rh, Ni\*, Pd) to five (Cu, Ag) as one proceeds across the  $3d$  and  $4d$  transition metal series. Mn is listed twice since the states with zero and three minority electrons added seem to be close in energy. Ni has an asterisk because it is an exception to the zero-three-five rule. The origin of this rule is almost certainly the grouping of states caused by the approximate cubic field of the oxygen ion distorted octahedron into a group of three and a group of two at higher energy coupled with the sharpness of these states as they cross the rather large gap in the minority DOS of  $\text{CrO}_2$ . Ni is the exception since its ground state is accompanied by an exceptionally large distortion of the oxygen octahedron that causes a relatively large splitting of the two “ $e_g$ ” states.

From the calculated DOS, the three “ $t_{2g}$ ” and two “ $e_g$ ” states are each spread over an energy range that varies from system to system, but is typically 2-3eV. Nevertheless, the calculated change in spin moment upon substitution is consistent with a picture in which these states have no dispersion. Thus the number of occupied minority d-states on the impurity is 0 ( $d^0$ - $d^3$  impurities) then jumps to 3 as all of the “ $t_{2g}$ ” minority impurity states ( $d^3$ - $d^6$  impurities) are occupied and finally jumps to 5 as the two “ $e_g$ ” minority impurity states are filled ( $d^7$  impurities). Part of the reason for this behavior is that the dispersion of the minority impurity states may be significantly decreased if they fall in the minority gap of the  $\text{CrO}_2$  where there are no d-states

with which to interact. This result, at least for this system, helps to reconcile the band and crystal field pictures of transition metal oxides.

### **Delocalized Moments**

Despite the fact that the moment rule discussed in the last section appears to be consistent with a picture of localized, dispersion-less minority electrons, within GGA-DFT, this picture seems to be significantly distorted for the majority electrons, especially for some of the 4d-impurities. In this section, we investigate the curious result mentioned in our discussion of Table II that although the moment associated with a Nb impurity is  $1\mu_B$ , as expected for a  $d^1$   $Nb^{4+}$  ion, this moment does not appear to reside on the Nb ion. Table II indicates that less than 7% of the moment associated with the impurity resides within a sphere of radius  $0.9\text{\AA}$  centered at the Nb ion. Figure 10, is a contour plot of the magnetization density for a slice through the cell parallel to an (001) plane. This slice cuts through the positions of a Cr ion and a Nb ion. It can be seen that the magnetization density almost vanishes in the region surrounding the Nb ion. It can also be seen that the magnetization near the O ions neighboring the Nb ion is increased compared those adjacent to a Cr ion. In fact, the increase in the magnetization in the vicinity of the neighboring O ions exceeds the magnetization in the vicinity of the Nb ion.

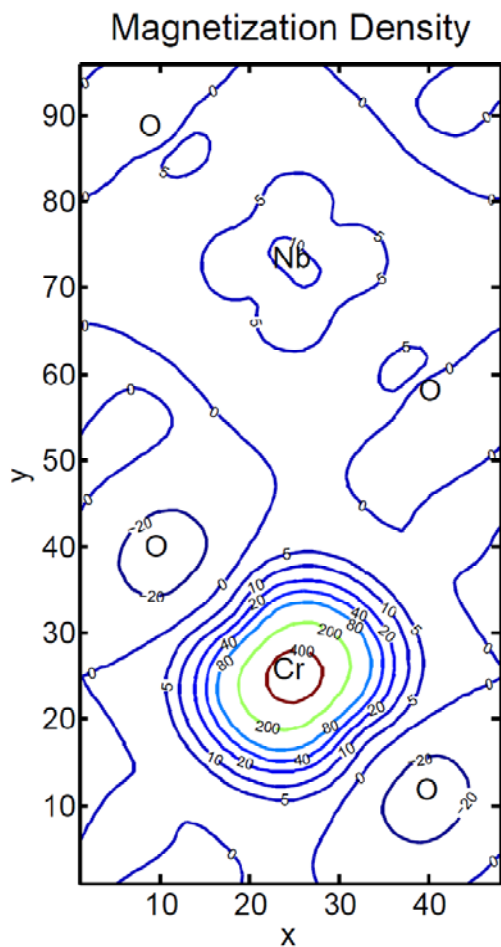


**Figure 10. (color online) Magnetization as a function of  $x$  and  $y$  for fixed  $z$ .  $z$  is parallel to the  $c$ -axis of the tetragonal cell. There is very little magnetization in the vicinity of the Nb ion, but enhanced magnetization on its neighboring O ions compared to O atoms bonded to Cr ions which have a negative magnetization density. The  $x$  and  $y$  axes of the cell are discretized into 48 and 96 units respectively. Each unit corresponds to 0.0094nm.**

Figure 11 shows the calculated difference between the magnetization for cells of composition  $\text{Cr}_7\text{NbO}_{16}$  and  $\text{Cr}_8\text{O}_{16}$ . In order to perform the subtraction, the magnetization density for  $\text{Cr}_8\text{O}_{16}$  was calculated for the same coordinates used for  $\text{Cr}_7\text{NbO}_{16}$ , i.e. the relaxed cell as distorted by the impurity.

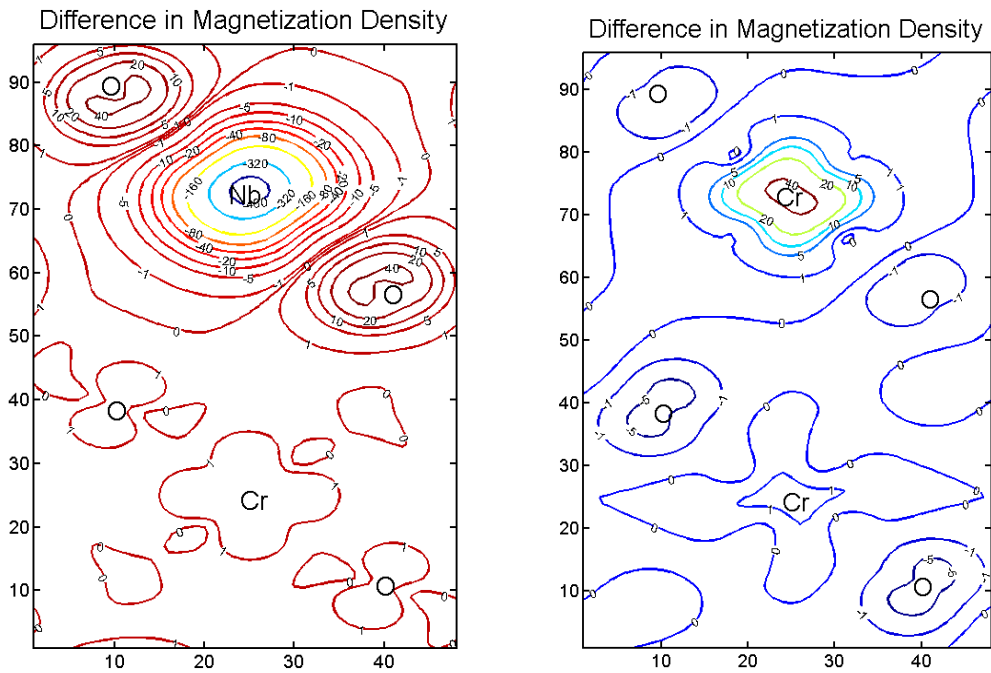


**Figure 11 (color online) Difference in magnetization between  $\text{Cr}_8\text{O}_{16}$  and  $\text{Cr}_7\text{NbO}_{16}$  for two cuts through the supercell for fixed  $z$ . The left panel shows the same cut as in figure 10. The elimination of the magnetization on the Nb site (difference is negative) and its enhancement on neighboring O ions can be seen. The right panel shows the difference in magnetization for a cut through a plane parallel to that of the left panel that does not contain a Nb substitution showing enhancement of the magnetization on the Cr ions immediately above and below the Nb ion (along the  $c$  axis) is enhanced. The  $x$  (short) and  $y$  (long) axes are discretized into 48 and 96 units respectively. Each unit is 0.0094nm.**

A similar effect can be seen for the magnetization of a Mo impurity in  $\text{CrO}_2$ . Although Mo is isoelectronic with Cr, and the calculated magnetic moment is unchanged when Mo is substituted for Cr, the calculated magnetization density is quite small in the vicinity of the Mo ion and the magnetization is enhanced on the Cr ions, especially the ones directly above and below the Mo along the  $c$ -axis.

### **Relevance of Correlation Effects**

In addition to the DFT-GGA calculations, we performed exploratory calculations using GGA+U with  $U=3.0$  eV and  $J=0.9$ eV on both the Cr and impurity ions for the Nb (minority  $d^0$ ), Ru (minority  $d^3$ ), and Ni (minority  $d^4$ ) impurities. As expected, the occupied states were moved down relative to unoccupied states. The Jahn-Teller splitting of the Ni  $e_g$  states is enhanced and our general picture of transition-metal-doped  $\text{CrO}_2$  remaining a half-metal with the moment rule as described above is reinforced. We have not conducted a full GGA+U investigation due to the difficulty in obtaining accurate U and J parameters and because GGA+U does not qualitatively change the picture presented by the parameter-less GGA calculations.

## **Conclusions**

We calculated the electronic structure of  $\text{CrO}_2$  with  $3d$  and  $4d$  transition metal ions as impurities. All of the considered systems were relaxed structurally. From our calculations, it can be seen that rutile  $\text{CrO}_2$  remains a half-metal when impurity elements are substituted for Cr forming  $\text{Cr}_{0.875}\text{Z}_{0.125}\text{O}_2$ . We find that the net change in spin magnetic moment can be understood in terms of a picture in which 0 ( $d^0$ - $d^3$  impurities), 3 ( $d^3$ - $d^6$  impurities) or 5 ( $d^7$  impurities) electrons from the impurity occupy the minority spin channel. This causes the net impurity moment to align antiferromagnetically with the Cr moments when the impurity has more than 3 valence electrons (the FM and AFM configurations are nearly degenerate in Mn).

We find a surprising result for the 4d substitutions Nb and Mo, which yield a total moment consistent with the notion that the Nb has a moment of  $1\mu_B$  and the Mo a moment of  $2\mu_B$ ; yet, a detailed study of the magnetization shows that there is only a very small moment on the Mo ion and even less on the Nb. These substitutions will have a profound effect upon the electronic states at the Fermi energy which remain fully spin-polarized. These unexpected

effects may offer the opportunity to engineer rutile-based heterostructures with modified transport properties and exchange interactions.

### **Acknowledgements**

The authors greatly appreciated input from Dr. Claudia Mewes of the MINT Center who read the paper and discussed various aspects with us. Some of the calculations were performed on the University of Alabama High-Performance Cluster. We also thank Professors Arunava Gupta and Patrick LeClair for helpful suggestions. This work was supported by the following grants: NSF MRSEC Grant No. 0213985 and NSF Rutiles project Grant No. 0706280, NSF Career award No. 0952929.

### **References**

- 1) Arunava Gupta (*private communication*)
- 2) H.W. Verleur, A.S. Barker, C.N. Berglund, Phys. Rev. 172 788 (1968).
- 3) K. Schwarz, J. Phys. F: Met. Phys. 16, L211 (1986)
- 4) V. Eyert, *Annalen Der Physik* 11, 650 (2002)
- 5) K. B. Chetry, H. Sims, W. H. Butler, and A. Gupta, Phys. Rev. B **84**, 054438 (2011).
- 6) M. E. Williams, W. H. Butler, C. K. Mewes, H. Sims, M. Chshiev, and S. K. Sarker, J. Appl. Phys. 105 07E510 (2009).
- 7) J.P. Perdew, in Electronic Structure of Solids 1991, edited by P. Ziesche and H. Eschrig (Akademie Verlag, Berlin, 1991), p 11

- 8) J.P. Perdew, K.Burke, and M.Ernzerhof Phys. Rev. Lett. 77, 3865 (1996)
- 9) G. Kresse and J. Furthmüller, Comput. Mater. Sci. 6, 15 (1996).
- 10) G. Kresse and D. Joubert, Phys. Rev. B 59, 1758 (1999).
- 11) H. J. Monkhorst, J. D. Pack, Phys. Rev. B **13**, 5188 (1976).
- 12) J. Je and S. B. Sinnott, J. Am. Ceram. Soc. 88, 737 (2005).
- 13) B. Martínez, J. Fontcuberta, M. J. Martínez-Lopez and J. A. Alonso, J. Appl. Phys. **87**, 6019 (2000).
- 14) H.A. Jahn and E. Teller, *Proc. R. Soc. London A* 161 220 (1937); H.A. Jahn, *Proc. R. Soc. Lond. A* 164 117 (1938).